VIRTUAL TESTING OF HONEYCOMB SANDWICH STRUCTURES WITH MULTIPLE LOAD INTRODUCTION POINTS

Lukas Schwan[a], Johann Schwenke[a], Tobias S. Hartwich[a], Dieter Krause[a]

a: Institute of Product Development and Mechanical Engineering Design, Hamburg University of Technology (TUHH) – lukas.schwan@tuhh.de

Abstract: *In Nomex honeycomb sandwich structures, inserts are often used for local load introduction. In the surroundings of the inserts, complicated stress conditions occur, which can often lead to local failure of the structure. Due to design measures, several inserts often have to be positioned next to each other, which can lead to interferences of the stress fields, reducing the load-bearing capacity of the individual inserts. For such cases, only rough reduction factors are specified in the ESA insert design handbook, which can lead to large safety factors. To predict the influence of the positioning of two inserts and to minimize oversizing, pull-out tests as well insert proximity tests are carried out. Respective virtual models are build-up for further numerical investigations.*

Keywords: virtual testing; Nomex honeycomb; insert proximity test; multiple load introduction points

1. Introduction

In aircraft cabins, sandwich structures with Nomex honeycomb core are frequently used due to their very good weight-specific properties [1]. Since the core is not suitable for local load transfer, local stiffeners in the form of inserts are introduced into the structure with an adhesive compound, so-called potting [1–3]. In addition to the layered structure of the sandwich composite and the anisotropic material behavior of the constituents, complicated stress states arise due to large stiffness changes in the area of the load introduction elements [1]. For design reasons, often multiple inserts must be used to introduce loads into the structure, which can lead to an overlapping of their stress fields [3]. This can result in a reduction of the load-bearing capacity of the individual inserts. In the Insert Design Handbook (IDH) [3], analytical equations are given to determine not only the load-bearing capacity of individual inserts but also interference coefficients, which indicate reductions in the load-bearing capacity of the inserts. In the case of two inserts loaded in the same direction, a distinction between *close* and *distant* inserts according to Eq. (1) is made, where *a* denotes the distance between the insert centers and b_{p1}, b_{p2} describe the respective potting radii. If the inequation is fulfilled, the inserts are classified as *close* and the interference coefficient η_{IS1} for insert 1 can be calculated according to Eq. (2). If the same inserts are used, the interference coefficients are the same ($\eta_{IS1} = \eta_{IS2}$), otherwise the IDH [3] gives further equations for the determination of η_{IS2}. If the insert distance *a* is greater than the term given in Eq. (1), the inserts are classified as *distant* and there is no reduction in the load-bearing capacity ($\eta_{IS1} = \eta_{IS2} = 1$).

$$a \leq 5(b_{p1} + b_{p2}) \tag{1}$$

$$\eta_{IS1} = \frac{b_{p1}/b_{p2}}{1+b_{p1}/b_{p2}} \left(1 + \frac{a}{5 \cdot b_{p1}} \cdot \frac{1}{b_{p1}/b_{p2}}\right) \tag{2}$$

  doi:10.5075/epfl-298799_978-2-9701614-0-0

However, these are approximate and conservative equations [4, 5] that do not fully exploit the lightweight design potential and lead to over-dimensioning. Detailed numerical meso-models based on the finite element method (FEM), which are hierarchically structured, have been established in research as an alternative to the analytical equations [6–8]. With such FEM-models, for example, it is possible to predict the structural behavior of Nomex honeycomb sandwich structures in the pull-out test [4, 9, 10]. Corresponding numerical and experimental results for multiple inserts, like the insert proximity test proposed in the IDH [3], could not be found in the state of the art. Only Schwenke and Krause [11] have numerically shown an optimization for multiple load introduction points.

In this paper, a realization of a test setup for the insert proximity test as well as corresponding test results are shown for the first time. Based on the pull-out test, detailed numerical models are further implemented and extended to the insert proximity test. The experimental results are complemented by numerical studies to generate knowledge about the load introduction across multiple inserts and to minimize over-dimensioning in the design of insert groups.

2. Materials

The presented materials are used for the pull-out tests as well as the insert proximity tests. The partially potted insert configuration used is shown in *Figure 1* and is typically used in aircraft cabins. The total panel thickness is 20 mm and a Nomex honeycomb core from the manufacturer Euro-Composites with a cell size of 3.2 mm and a density of 48 kg/mm² according to the Airbus standard ABS5035-A4 is used. Two layers of glass fiber fabric reinforced phenolic resin prepreg to Airbus standard ABS5047-07 are placed on each side of the core. The SL607-3-6S inserts are cold-bonded into the structure with Scotch-Weld 9323 adhesive. The potting height is 17 mm.

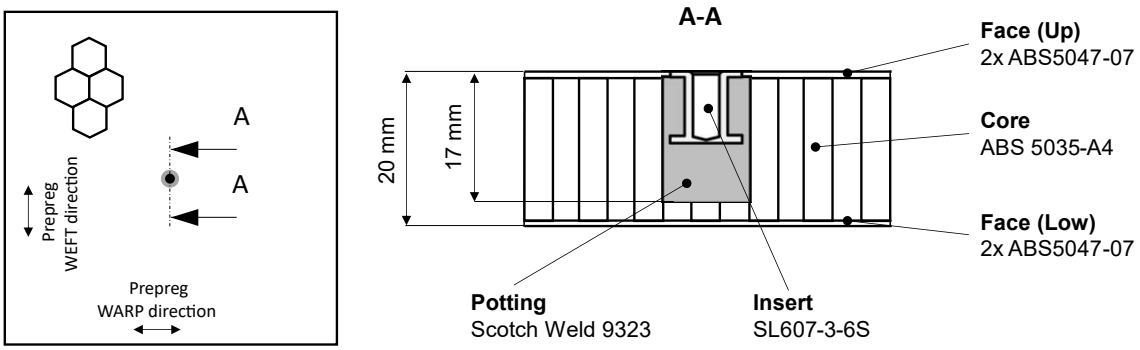

Figure 1. Used materials for the pull-out tests and the insert proximity tests.

3. Pull-out test

First, pull-out tests are performed to implement a numerical model, which will be extended to the insert proximity test.

3.1 Experimental study

The tests are performed following the recommendations from the IDH [3] and three specimens with a specimen size of 100 x 100 mm are tested. The cutout diameter is 70 mm and a loading rate of 2 mm/min is used. The tests are carried out on a Galdabini Quasar 100 universal testing machine, while the force is measured using an HBM S9M-10 kN load cell and the displacement is measured via machine crosshead. The experimental setup is shown in *Figure 2*.

  doi:10.5075/epfl-298799_978-2-9701614-0-0

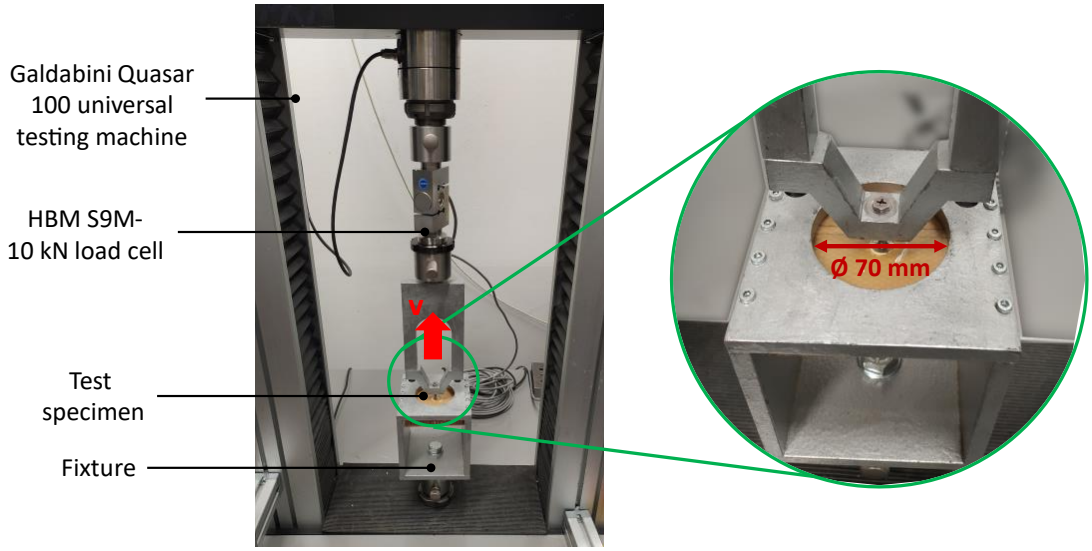

Figure 2. Experimental setup for the pull-out test.

3.2 Numerical study

The FEM-model of the pull-out test is implemented as a quarter model with a meso-core and the FEM solver Abaqus/Explicit is used. The meshed model is shown in *Figure 3*, using the modeling approaches and material models of Seemann [12].

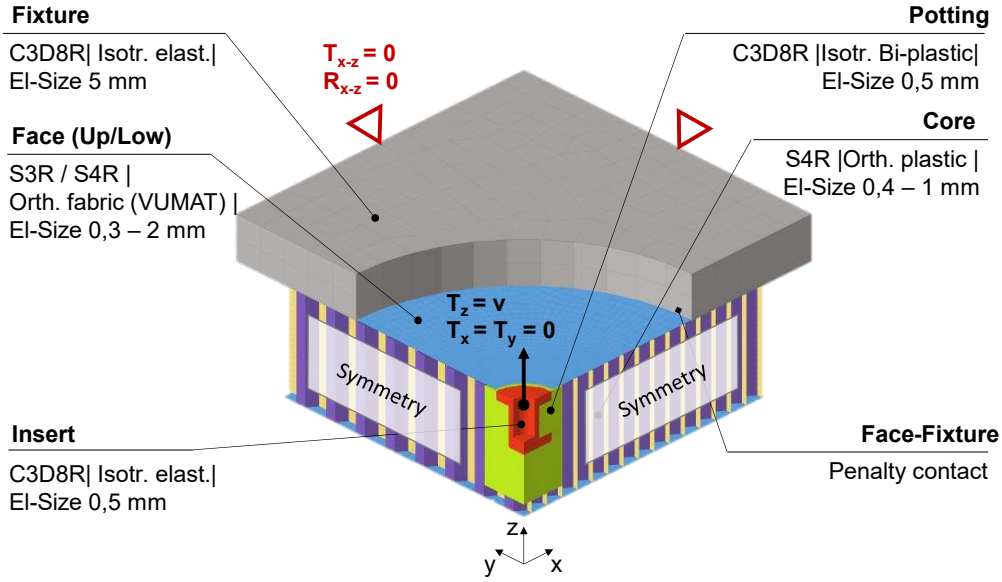

Figure 3. Meso model of the pull-out test modeled according to Seemann and Krause [9].

In particular, to predict the nonlinear behavior of the sandwich structure in the pull-out test, the shear buckling of the core as initial damage mechanism must be adequately modeled [3, 13]. To implement this with meso-models, the material properties of the phenolic resin impregnated Nomex paper type 412 are of great importance [14]. Following Seemann and Krause [14], an orthotropic plastic material model with Hashin failure criterion is used for modeling. While the elastic material parameters as well as the compressive and shear strengths are kept according to Seemann and Krause [14], the tensile strength in M- and X-direction is reduced as part of the model calibration in order to reduce the deviation from the tensile strengths reported in the

  doi:10.5075/epfl-298799_978-2-9701614-0-0

literature [15, 16]. Furthermore, various parameter and sensitivity analyses are performed to calibrate the fracture energies of the phenolic resin impregnated Nomex paper. The calibrated material parameters of the core are summarized in *Table 1*.

Table 1: Calibrated material parameters for the phenolic resin impregnated Nomex paper.

E_1	5.000 MPa	Longitudinal tensile strength, δ_{1t}	75 MPa	Longitudinal tensile fracture energy, G_{1t}	30 N/mm
E_2	4.000 MPa	Longitudinal compression strength, δ_{1c}	105 MPa	Longitudinal compression fracture energy, G_{1c}	10 kN/mm
G_{12}	1.450 MPa	Transverse tensile strength, δ_{2t}	30 MPa	Transverse tensile fracture energy, G_{2t}	20 N/mm
υ_{12}	0,2	Transverse compression strength, δ_{2c}	90 MPa	Transverse compression fracture energy, G_{2c}	10 kN/mm
		Shear strength, δ_{12}	44 MPa		

3.3 Results

Figure 4 (a) shows the results of the experimental study and the numerical simulation, with the test stiffness extracted from the test data. Initially, the sandwich structure exhibits linear elastic behavior, whereupon shear buckling of the core occurs, giving the force-displacement curve its characteristic progressive course until total failure of the structure occurs. Further, partial delamination and failure of the face sheets occur, which can also be detected in the tested specimens in *Figure 4 (b).* The results of the numerical simulation agree well with those of the physical tests, although the initial shear buckling is slightly overestimated in the virtual model.

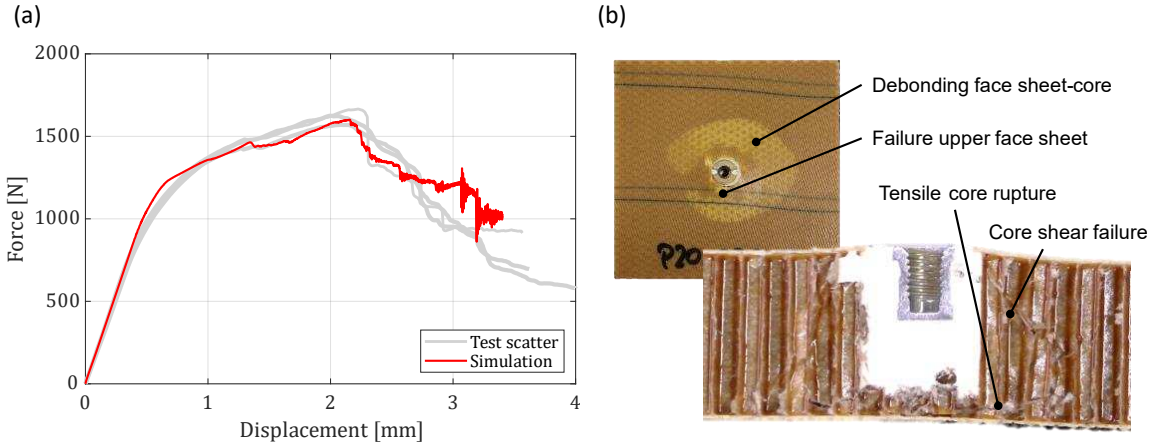

Figure 4: Results of the experimental study and numerical simulation (a); Damage mechanisms occurring in the physical test (b).

4. Insert proximity test

After the pull-out test has been successfully modeled numerically, experimental tests as well as numerical studies on the insert proximity test are performed.

4.1 Experimental study

The insert proximity tests are performed on the same universal testing machine with the same traverse speed as the pull-out tests. The optical 3D measuring system ARAMIS Adjustable from GOM is used for displacement measurement. The test setup is shown in *Figure 5*. A cutout

diameter of 140 mm and a specimen size of 200 x 200 mm are selected. Also, a universal joint is used for force application to prevent the introduction of transverse forces into the specimen. A steel plate with drilling holes is utilized for the testing of the different insert configurations. Furthermore, 14 mm, 50 mm and 80 mm are chosen as insert distances in W-Direction (cf. *Figure 5*). For the three chosen distances according to the analytical equations from the IDH [3] there is a slight, a moderate and no influence on the load-bearing capacity as a result of the superposition of the insert stress fields. Three specimens of each configuration are tested.

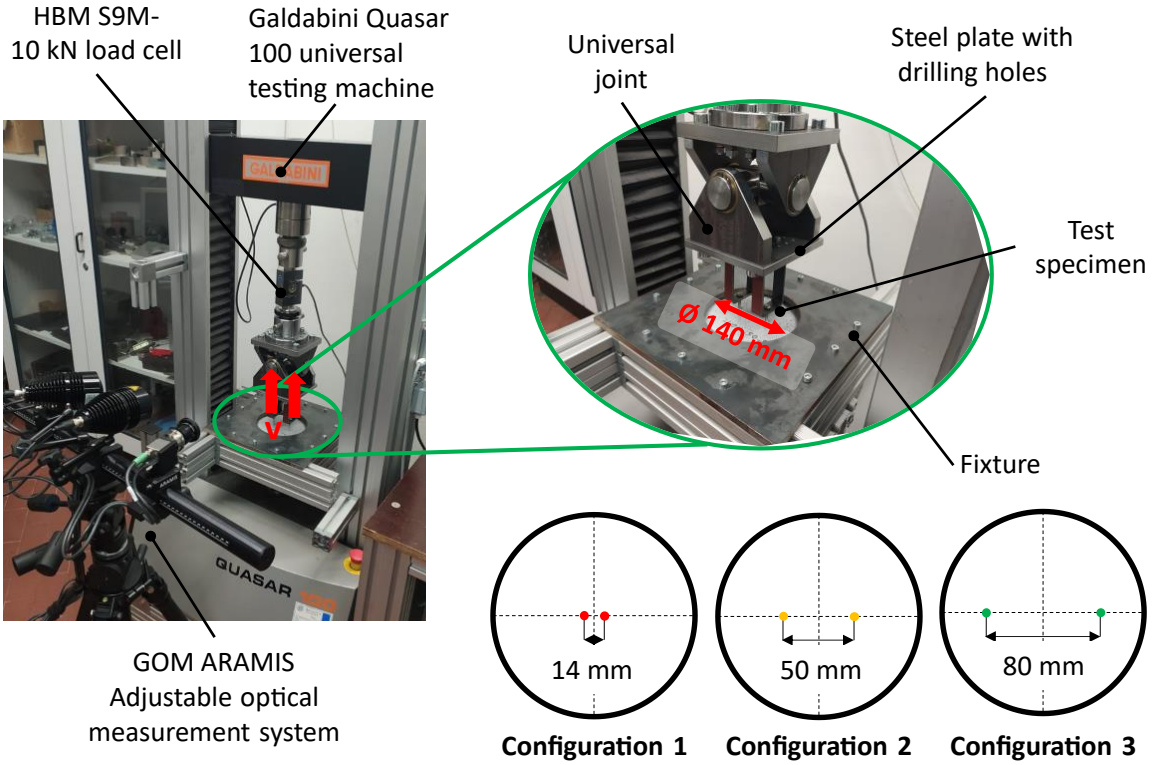

Figure 5. Test setup for the insert proximity test and different test configurations.

4.2 Numerical study

Two different models are implemented as part of the numerical study. In addition to a hybrid model, which is set up for the prediction of the progressive damage behavior, a solid model is also set up in order to be able to calculate different insert positions in a computationally efficient manner. With the exception of the solid core, both models are implemented as a quarter model with the same element sizes and material models as the pull-out model from chapter 3.2. To save computation time due to the larger sample size, the core in the hybrid model is modeled at a radius of 20 mm around the insert using a meso core in order to be able to represent the shear buckling. At a further distance, a solid core with an element size of 5 mm and an orthotropic plastic material model according to Seemann [12] is used, which is able to reproduce the elastic behavior of the core. The two cores were connected by a tied contact. When exploiting the symmetry in the quarter model using a meso or hybrid modeling approach, in which the geometry of the honeycomb core is represented, the resulting potting geometry has an effect on the shear stresses that occur in the individual honeycomb cell walls and thus on the resulting pull-out force [17]. Thus, the influence of the positioning of the inserts cannot be

  doi:10.5075/epfl-298799_978-2-9701614-0-0

studied in isolation due to its correlation with the resulting potting geometry. For this purpose, a solid model is implemented in which the honeycomb is not geometrically represented. Although the progressive damage behavior cannot be adequately represented by this, the solid models are suitable for determining the pull-out forces. The solid model is used to simulate insert distances between 14-120 mm in 10 mm increments in the L- and W-direction.

4.3 Results

Figure 6 (a-c) shows the results of the experimental tests for the different insert distances and the results of the corresponding numerical simulation with the hybrid model. In addition, in *Figure 6 (d)* a 50 mm specimen is shown, in which similar failure mechanisms as in the pull-out test can be identified. Overall, the results of the hybrid models are within the scatter of the tests and represent the progressive damage behavior of the structure well. While the maximum force for the 14 mm configuration is lower than the maximum forces of the 50 mm and the 80 mm configurations, a reduced strength for the 80 mm configuration compared to the 50 mm configuration can be observed.

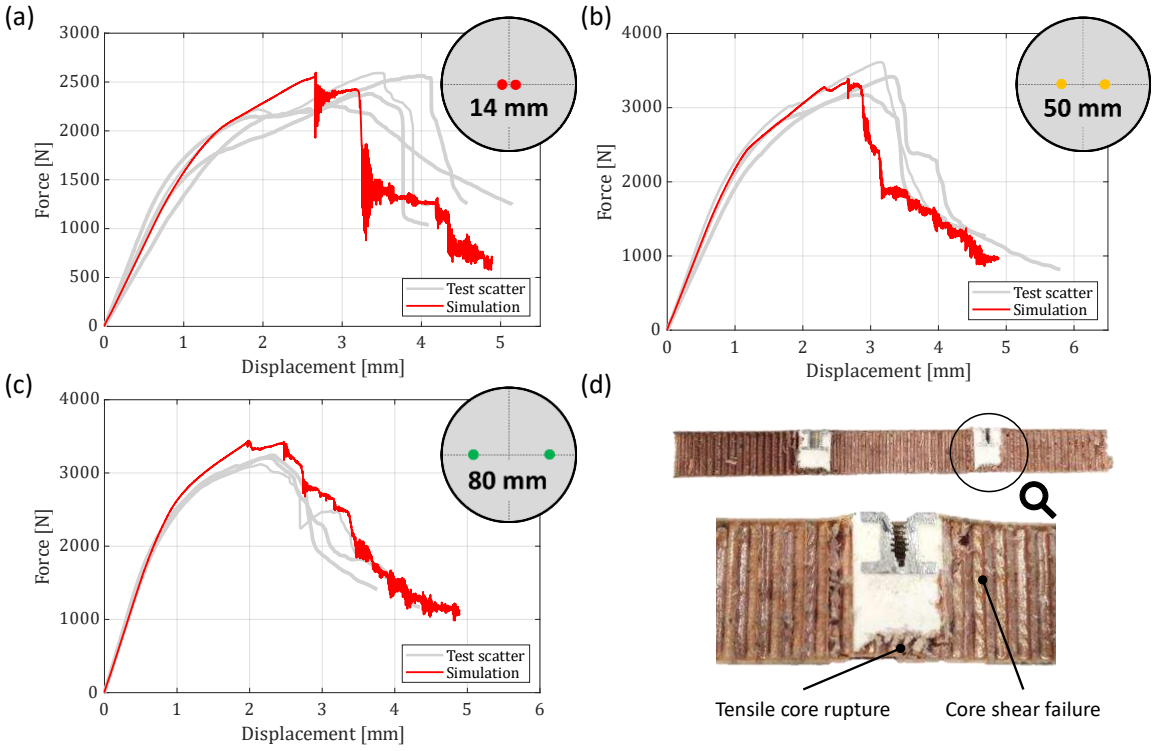

Figure 6. Results of the experiments and numerical simulations for different insert distances (a-c); Damage mechanisms occurring in the core in physical test of the 50 mm configuration (d).

The evaluation of the results of the solid model in smaller distance increments supports these findings from the physical tests and the numerical investigations with the hybrid model. *Figure 7 (a)* shows the simulatively determined as well as the analytically determined interference coefficients over the insert distance. While the analytic interference coefficients have been calculated according to Eq. (1) and Eq. (2), for the simulatively calculation the Equation from *Figure 7 (a)* is applied assuming an even load distribution in the insert proximity test. As reference, a solid model with a single insert is implemented for a pull-out test with a cutout diameter of 140 mm. The corresponding pull-out forces are afterward determined in the

  doi:10.5075/epfl-298799_978-2-9701614-0-0

force-displacement diagram by intersection of the simulation from the 5 %-regression line in the tests. In addition to the fact that no distinction is made between the L- and W- directions in the IDH [3], it is apparent that the analytical equations from the IDH [3] are conservative for insert distances until 40 mm compared to the simulatively determined interference coefficients. In the simulation, there is also a clear difference in the L- and W- directions which is due to the fact that the stress distribution in the core assumes an oval shape because of the stronger double walls (exemplarily shown in *Figure 7* (b)). As a consequence, the overlapping area of the stress fields with an insert positioning along the W-direction is smaller than in the L-direction. After a plateau is reached, the interference coefficients in the simulation reduce again. This can be attributed to restraint effects since parts of the stress fields of the inserts are now placed under the clamping. Such effects are not considered in the analytical equations in the IDH [3].

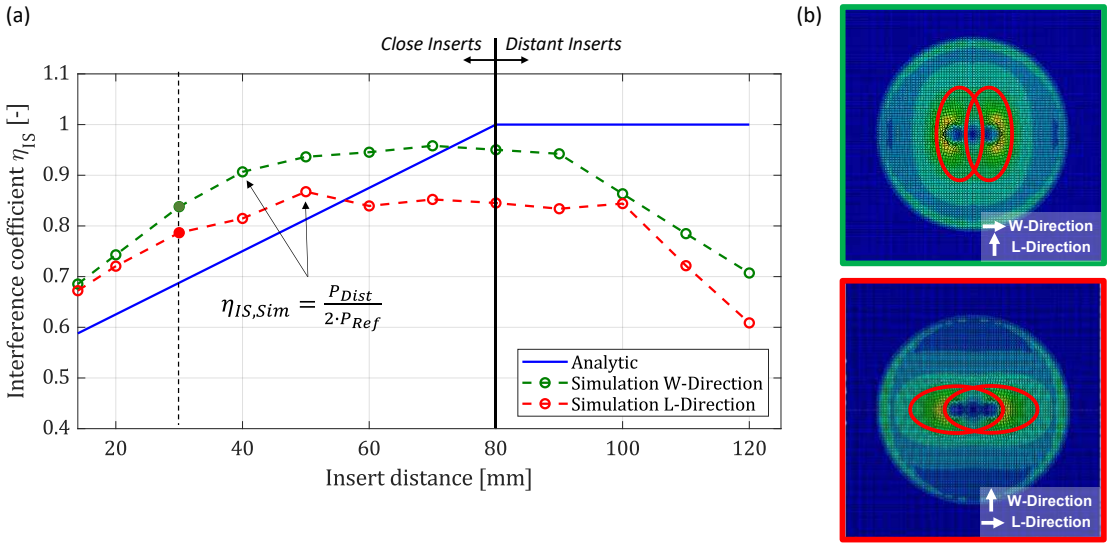

Figure 7. Interference coefficients over different insert distances (a); Stress fields for Insert distance of 30 mm in W-direction (green) and L-direction (red) (b).

5. Conclusion and outlook

If several inserts are loaded in the same direction, their stress fields can overlap, which leads to a reduction of their load-bearing capacities. In this paper, a detailed numerical model was implemented based on the pull-out test and was subsequently extended to the insert proximity test. Furthermore, test results of the insert proximity test for three different insert distances were shown. Using a hybrid modeling approach consisting of a meso and a solid core, the progressive damage behavior of the sandwich structure from the experiments could be accurately reproduced. Numerical studies of different insert distances with simplified solid models further show that the core orientation has a large influence on the resulting interference coefficients. Overall, the virtual models developed lead to an improvement in the design with multiple load introduction elements and result in a more accurate prediction compared to the analytical equations in the IDH. In further research, additional simulations for insert groups with asymmetric load introduction can be investigated. In order to ensure a successive transferability to the product level and to improve the numerical design, it is further planned to increase the structural complexity and to investigate larger structures.

  doi:10.5075/epfl-298799_978-2-9701614-0-0

Acknowledgements

The acknowledgements being relevant for this contribution are based on the research projects *EFFEKT (20D1927D); DEPOSE (20Q1905)* and *CabinJoint (20Q1904B)* supported by the Federal Ministry for economic Affairs and Climate Actions (BMWK) on the basis of a decision by the German Bundestag.

6. References

[1] Zenkert D. *Handbook of Sandwich Construction*. Cradley Heath: EMAS; 1997.
[2] Bitzer T. *Honeycomb Technology*. Dordrecht: Springer; 1997.
[3] European Cooperation for Space Standardization - ECCS. ECSS-E-HB-32-22A: *Space Engineering Insert Design Handbook*. 2011.
[4] Heimbs S, Pein M. Failure behaviour of honeycomb sandwich corner joints and inserts. *Composite Structures*. 2009; 89(4): 575–88.
[5] Dios Rodríguez-Ramírez J de, Castanié B, Bouvet C. Insert of sandwich panels sizing through a failure mode map. *Composite Structures*. 2020; 234: 111724.
[6] Department of Defense. *Composite Material Handbook - Volume 3 Polymer matrix composites materials usage, design and analysis*. 1997.
[7] Schwan L, Hüttich P, Wegner M, Krause D. Procedure for the transferability of application specific boundary conditions for the testing of components and products. In: Krause D, Paetzold K, Wartzack S. (eds.) *Proceedings of the 32nd Symposium Design for X, DfX 2021, 27-28 September 2021, Tutzing, Germany.*
[8] Heyden E, Hartwich TS, Schwenke J, Krause D. Transferability of Boundary Conditions in Testing and Validation of Lightweight Structures. In: Krause D, Paetzold K, Wartzack S. (eds.) *Proceedings of the 30th Symposium Design for X, DfX 2019, 18-19 September 2019, Jesteburg, Germany.*
[9] Seemann R, Krause D. Numerical modelling of partially potted inserts in honeycomb sandwich panels under pull-out loading. *Composite Structures.* 2018; 203: 101–9.
[10] , Nguyen KH, Park YB, Kweon JH, Choi JH. Testing and modeling of Nomex™ honeycomb sandwich Panels with bolt insert. *Composites Part B: Engineering*. 2014; 56: 762–9.
[11] Schwenke J, Krause D. Optimization of load introduction points in sandwich structures with additively manufactured cores. *Design Science*. 2020; 6.
[12] Seemann R. *A Virtual Testing Approach for Honeycomb Sandwich Panel Joints in Aircraft Interior*. Berlin: Springer Berlin Heidelberg; 2020.
[13] Rodriguez-Ramirez JdD, Castanie B, Bouvet C. Experimental and numerical analysis of the shear nonlinear behaviour of Nomex honeycomb core: Application to insert sizing. *Composite Structures.* 2018; 193: 121–39.
[14] Seemann R, Krause D. Numerical modelling of Nomex honeycomb sandwich cores at meso-scale level. *Composite Structures.* 2017; 159: 702–18.
[15] Tsujii. Analysis of Mechanical Properties of Aramid Honeycomb Core. *Transactions of the Japan Society of Mechanical Engineers Series A*. 1995; 61(587): 1608-14.
[16] Roy R, Park S-J, Kweon J-H, Choi J-H. Characterization of Nomex honeycomb core constituent material mechanical properties. *Composite Structures.* 2014; 117: 255–66.
[17] Slimane S, Kebdani S, Boudjemai A, Slimane A. Effect of position of tension-loaded inserts on honeycomb panels used for space applications. *Int J Interact Des Manuf*. 2018; 12(2): 393–408.

  doi:10.5075/epfl-298799_978-2-9701614-0-0